An experimental and theoretical study on the electrostatic effect of an appended cationic group on electronic properties of aromatic systems†

Viviana Grosso,[a] Carlos Previtali,[a] Carlos A. Chesta,*[a] D. Mariano A. Vera*[b] and Adriana B. Pierini*[b]

Received 27th June 2007, Accepted 10th September 2007
First published as an Advance Article on the web 28th September 2007
DOI: 10.1039/b709751d

Tetraalkylammonium salts, characterized by an aromatic system pending from one of the alkyl chains, are taken as model systems to study the spectroscopic and redox properties of the aromatic centre under the field effects exerted by the charged group through alkyl bridges of varying length. The changes in the aromatic's redox properties, due to the net field effect and its different components, are interpreted on theoretical bases.

Introduction

Through-space Coulombic interactions between a remote unipole (or dipole) and a molecule can produce quantifiable changes in its reactivity.

In principle, the magnitude of the Coulombic effects depends on the unipolar charge–dipole moment, orientation of the dipole, distance between the reactive centre and the unipole (or dipole), and on the effective dielectric constant.[1] The importance of these electrostatic effects (or field effects) was first recognized by Bjerrum[2] and Kirkwood[3] and further investigated in more recent years in connection with the electrostatic catalysis in enzymes[4–10] and with the significant changes observed in the reactivity of organic molecules when exposed to the electric field exerted by remote ions. Remarkable examples of these effects are the enhancement of the rate of enolization of cationic ketones,[11] the changes on the regioselectivity and kinetics of the reductive cleavage of alkyl aryl ethers,[12] the modification of the photophysical and photochemical properties of diverse substrates absorbed in zeolites[13,14] and the changes observed in the photophysical and redox properties of a chromophore/fluorophore after metal complexation in crown-ether-based sensors.[15,16] However, despite this apparent interest, only a few studies involving experimental and theoretical analyses of these Coulombic effects have been reported.[8,13]

We report here a study on the field effects exerted by a tetraalkylammonium (TAA) group on the properties of a series of aromatic compounds. This study involves the spectroscopical and electrochemical characterization of the **c*n*Ar** salts in Chart 1 (**Ar** = aromatic chromophore, **c*n*** = carbon chain of *n* methylene units) and a comparison with the corresponding neutral derivatives, in which the $-(CH_2)_n-$TAA group has been replaced by H (or CH_3). All experiments were carried out in a polar solvent (acetonitrile) and at low concentrations of

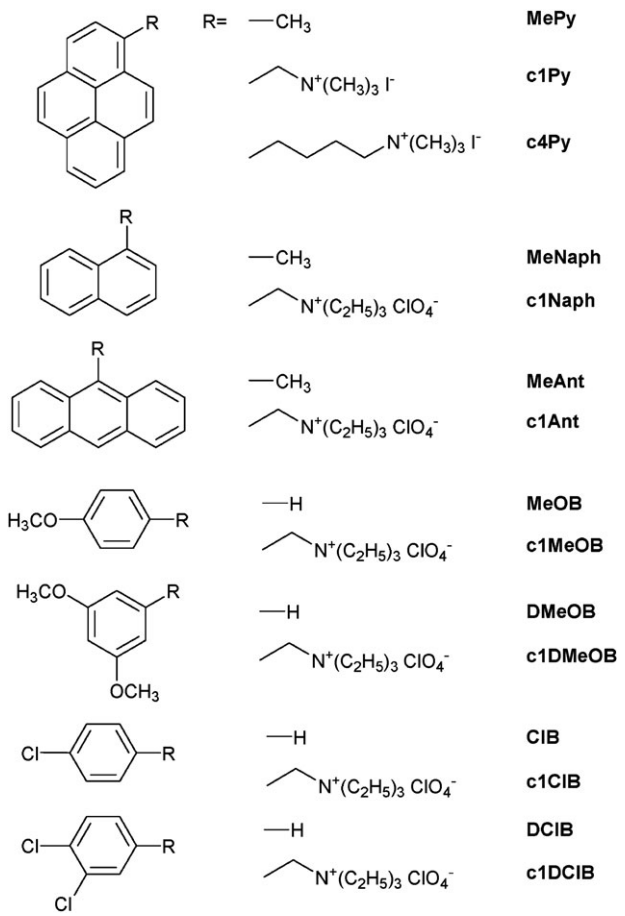

Chart 1

[a] *Departamento de Química, Universidad Nacional de Río Cuarto, 5800–Río Cuarto, Argentina. E-mail: chesta@exa.unrc.edu.ar*
[b] *INFIQC, Departamento de Química Orgánica, Facultad de Ciencias Químicas, Universidad Nacional de Córdoba, 5000–Córdoba, Argentina. E-mail: mariano@fcq.unc.edu.ar. E-mail: adriana@fcq.unc.edu.ar*

† Electronic supplementary information (ESI) available: Supplementary Figures to the experimental and theoretical subsections: KT calculations on the electron affinities and ionization potential of structurally related compounds. Additional models and whole summary of orbital energies for the whole species and models under study in gas phase and in PCM acetonitrile. DFT calculations details for the thermochemistries on Chart 2 for naphthalene, anthracene and pyrene series, including total energies in atomic units for each substrate and oxidized/reduced product both in gas phase and in acetonitrile. Details on the NBO analysis of the orbital interactions. Cartesian coordinates of main species and models under study. See DOI: 10.1039/b709751d

the salts ($<10^{-2}$ M). Under these experimental conditions the salts are expected to be completely dissociated, leaving the TAA group free to exert a strong Coulombic effect on the aromatic rings. Calculations using first-principles methods were carried out on several model systems to evaluate the nature and the magnitude of the effects produced by the charged group due to its electrostatic potential and to its electronic coupling through the alkyl bridge. We analyzed here the effects of the distance/orientation of the charge with respect to the chromophore, the role of the bridge itself, and the effect exerted by a polar solvent on the electrostatic effects.

Material and methods

Reagents

Acetonitrile (HPLC grade) was from Sintorgan. 1-(Chloromethyl)benzene (Aldrich, 97%), 1,3-dichloro-5-(chloromethyl)-benzene (Aldrich, 97%), 1-(chloromethyl)-4-methoxybenzene (Aldrich, 98%), 1-(chloromethyl)-3,5-dimethoxybenzene (Aldrich, 99%), 9-(chloromethyl)anthracene (Aldrich, 98 + %), and 1-(chloromethyl)naphthalene (Aldrich, 90%) were used as received. Triethylamine (Aldrich, 98%) was distilled prior to use.

Synthesis

c1Py and **c4Py** were provided by Molecular Probes. **c1Naph** was prepared as previously reported.[17] The other salts in Chart 1 were prepared from the corresponding 1-(chloromethyl) aromatics and triethylamine according to an adaptation of the procedure reported by Arnold *et al.*[18] Typically, 2 g of the halide and 25 mL of freshly distilled triethylamine were refluxed with stirring for 8 hours. The salt was filtered out, dissolved in water, and was then precipitated out as the perchlorate salt by addition of a saturated aqueous solution of $NaClO_4$. Finally, the salts were recrystallized from ethyl acetate and vacuum dried at 45 °C for 24 hours. Yields varied from 60–70%.

c1ClB. ^{1}H NMR (Cl_3DC, TMS) δ/ppm: 1.44 (t, 9H, $-CH_3$), 3.26 (q, 6H, $-CH_2-$), 4.47 (s, 2H, $-CH_2-$, benzylic), 7.26 and 7.43 (s, aromatics, 4H). Elem. anal. calculated for $C_{13}H_{21}Cl_2NO_4$: C: 47.86%, H: 6.49%, Cl: 21.74%, N: 4.29%. Found: C: 47.95%, H: 6.43%, N: 4.36%. The IR (KBr) showed two pronounced absorptions at 1090 and 620 cm^{-1}, both characteristic of the ClO_4^- ion.

c1DClB. ^{1}H NMR (Cl_3DC, TMS) δ/ppm: 1.45 (t, 9H, $-CH_3$), 3.29 (q, 6H, $-CH_2-$), 4.50 (s, 2H, $-CH_2-$, benzylic), 7.4–7.5 (m, 3H, aromatic). Elem. anal. calculated for $C_{13}H_{20}Cl_3NO_4$: C: 43.29%, H: 5.6%, Cl: 29.49%, N: 3.88%. Found: C: 43.26%, H: 5.7%, N: 3.85%. IR (KBr): 1090 and 620 cm^{-1}.

c1MeOB. ^{1}H NMR (Cl_3DC, TMS) δ/ppm: 1.45 (t, 9H, $-CH_3$), 3.25 (q, 6H, $-CH_2-$), 3.85 (s, 3H, $-OCH_3$), 4.38 (s, 2H, $-CH_2-$, benzylic), 7.4–7.5 (m, 4H, aromatic). Elem. anal. calculated for $C_{14}H_{24}ClNO_5$: C: 52.25%, H: 7.5%, Cl: 11.02%, N: 4.35%. Found: C: 52.22%, H: 7.4%, N: 4.41%. IR (KBr): 1090 and 620 cm^{-1}.

c1DMeOB. ^{1}H NMR (Cl_3DC, TMS) δ/ppm: 1.44 (t, 9H, $-CH_3$), 3.26 (q, 6H, $-CH_2-$), 3.88 (s, 6H, $-OCH_3$), 4.30 (s, 2H, $-CH_2-$, benzylic), 6.7 (m, 3H, aromatic). Elem. anal. calculated for $C_{15}H_{26}ClNO_6$: C: 51.21%, H: 7.5%, Cl: 10.08%, N: 3.98%. Found: C: 51.20%, H: 7.6%, N: 3.95%. IR (KBr): 1090 and 620 cm^{-1}.

c1Ant. ^{1}H NMR (Cl_3DC, TMS) δ/ppm: 1.45 (t, 9H), 3.28 (q, 6H), 4.87 (s, 2H), 7.3–7.7 (m, 9H). Elem. anal. calculated for $C_{21}H_{26}ClNO_4$: C: 64.36%, H: 6.69%, Cl: 9.05%, N: 3.57%. Found: C: 64.22%, H: 6.62%, N: 3.52%. IR (KBr): 1090 and 620 cm^{-1}.

Instrumental

Absorption spectra were recorded using a HP 8453 UV-visible spectrophotometer. IR spectra were obtained using a Nicolet Impact 400 spectrophotometer. ^{1}H NMR spectra were recorded on a Brucker 200 MHz nuclear magnetic resonance spectrometer.

Stationary fluorescence experiments were carried out using a Spex Fluoromax spectrofluorometer. All measurements were performed in deoxygenated solutions at (298 ± 1) K. Lifetime measurements were performed by using the time-correlated single photon counting technique (TCSPC) with an Edinburgh Instruments OB900 apparatus.

Cyclic voltammetry experiments were done using an EG & G Princeton Applied Research PAR-273 potentiostat–galvanostat. The current and potentials were registered either on an EG & G PAR RE 0150 XY recorder or with a Keithley 194A high speed voltmeter connected to a computer. A conventional three-compartment Pyrex cell was used. A Pt microelectrode (d = 25 μm) or a standard Pt electrode (A = 0.23 cm^2) were used as working electrodes. All the potentials were measured with reference to the saturated calomel electrode (SCE). All redox potentials were determined in acetonitrile using tetrabutylammonium perchlorate (0.1 M) as the supporting electrolyte. Depending on the experiment, the concentration of the salts was varied between 10^{-2}–10^{-3} M.

Computational details

The conformational space of the compounds shown in Chart 1 was first explored at the semiempirical AM1 level and characterized by means of normal analysis. Next, they were optimized at the HF/6-31G* level. A series of **c*n*Naph** salts (n = 1–16) was also calculated. Apart from the structures having a totally *gauche* chain (**c*n*Ar** series, where the distance varies with ***n***), other conformers (see below) were also optimized for exploring the effect of changing the orientation of the charged group with respect to the aromatic ring.

The difference in energy between the HOMOs of the **c*n*Ar–MeAr** pair and the energy difference between their LUMOs were evaluated. These energy differences are referred to as the Koopman's ionization potential (ΔI) and electron affinity shifts (ΔE_A), respectively, and are expected to give a first estimate of the modifications in the donor and acceptor capabilities due to the presence of the charged group in the absence of a solvent.

The Koopman's theorem (KT)[19] estimation of these shifts is expected to give a linear correlation with the actual change of

the gas-phase donor/acceptor properties of the systems[20–23] and it was indeed reasonable as confirmed by two independent criteria: (i) linear correlations of KT values with experimental I or E_A values for structurally related compounds[20] (the details are included as ESI†) and (ii) highly correlated calculations of thermodynamic values of these properties in selected systems (*i.e.* by computing the total energy of the oxidized and reduced forms of the **c*n*Ar–MeAr** pair, see below).

For the naphthalene, anthracene and pyrene derivatives on Chart 1, the shifts in the standard oxidation or reduction potentials were evaluated through the thermodynamic cycle on Chart 2 at the B3LYP/6-31 + G** // B3LYP/6-31G* level of theory.[24,25] Further corrections were obtained at the B3LYP/6-311 + + G(2d,p) // B3LYP/6-31G* level.[26,27] The potentials were evaluated in acetonitrile (the solvent used in the electrochemical and spectroscopic studies). This solvent was modeled by means of Tomasi's polarized continuum model (PCM), as implemented in Gaussian 98;[28,29] the solvation energies were obtained using the gas-phase equilibrium geometries.

The charge localization and the electrostatic potential calculations (ESP) were done by using the Merz–Singh–Kollman (MK) scheme.[30] Models to evaluate the effect of an external (non-bonded) electric field on the unsubstituted aromatics were considered, by combining the **MeAr** molecule with an array of point charges. Under this approach, the $-NMe_3^+$ group was modeled by a set of atomic point charges positioned at the TAA atomic coordinates and chosen to fit its electrostatic potential (ESP) in the real salt.[31] For some species under study, the interaction between the aromatic π system and the substituent was analyzed using localized natural bonding orbitals, with the NBO 3.1 standard program from the Gaussian 98 package.[28,32]

Results and discussion

Characterization of the salts

The shape and energy (wavelength) of the maxima of the absorption (and emission, when detected) spectra of the salts do not differ significantly from those of the **MeAr** aromatics. The absorption and emission spectra of **c1Naph** in acetonitrile are shown in Fig. 1. Approximated values of the salt's singlet–singlet excited state energies (E_{00}) were estimated from the wavelength of the 0–0 absorption/emission vibronic bands as shown in Fig. 1 and collected in Table 1.

In agreement with earlier studies on the photochemistry of structurally related compounds,[33,34] some of the salts studied here photodecompose upon irradiation. The decomposition rates depend on the nature of the aromatic chromophore. While salts **c4Py** and **c1Py** are photostable, **c1Naph** and **c1Ant** quickly decompose to produce 1-methylnaphthalene and 9-methylanthracene, respectively. Both products were detected by GC-mass spectroscopy upon photolysis of the salts in acetonitrile–2-propanol (9 : 1) (Fig. S1 in ESI†). The lack of emission from **c1Ant** indicates the particular importance of this photodecomposition process for the anthracene derivative. The fluorescence lifetimes (τ_0) measured in acetonitrile for the pyrene, naphthalene and anthracene compounds are collected in Table 1.

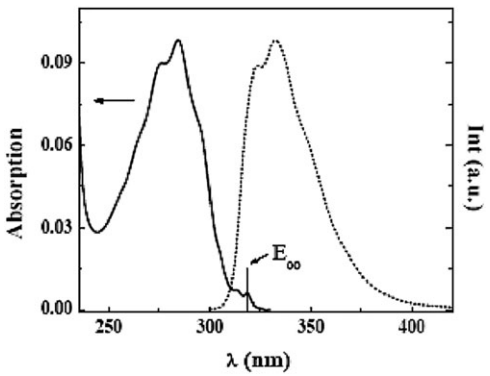

Fig. 1 Absorption (left) and fluorescence spectra (right) of 1.2×10^{-5} M **c1Naph** in acetonitrile at 298 K.

Fig. 2 shows the voltagrams obtained for the reduction of **c1Py** using either a Pt microelectrode (d = 25 μm) (a) or a standard Pt electrode (A = 0.23 cm^2) (b). As it can be concluded from voltagram (a) the reduction of the salt takes place at ~ −1.4 V. Although a similar potential can be guessed from voltagram (b), the lack of a reverse wave shows the irreversibility of the reductive process. It can be concluded that the anion radical of **c1Py** undergoes fast secondary reactions and, therefore, that the potential measured from the experiments in Fig. 2 does not represent a formal reduction potential (E°) value. Similar behaviours were observed for all the salts studied: for both types of processes, oxidations and reductions. Thus, the oxidation (E_{ox}) and the reduction (E_{red}) potentials reported in Table 1 could depart from the standard values by ~0.06–0.07 V.[38]

The oxidation potentials of salts **c1Py**, **c1Naph**, **c1Ant** and **c1DMeOB** are more anodic that those observed for the unsubstituted (or methylsubstituted) compounds. The relative

Table 1 Redox potentials in V *vs.* SCE, singlet–singlet excited state energies (E_{oo}) and emission lifetimes (τ_o) of the compounds studied in acetonitrile at 298 K

Compound	$E_{Ar^+\bullet/Ar}$/ eV [d]	$E_{Ar/Ar^-\bullet}$/ eV	E_{00}/ eV	τ_0/ ns
Pyrene[a]	1.20	−2.10	3.34	350
c4Py	1.25	−2.10	3.34	210
c1Py	1.52	−1.40	~3.30	62
Naphthalene[a]	1.43	−2.62	3.95	96
c1Naph	1.85	−2.03	~3.90	3.4
Anthracene[a]	1.09	−1.98	3.31	3.9
c1Ant	1.35	−1.27	~3.27	—
Methoxybenzene[b]	1.76	—	—	—
c1MeOB	>2.20	—	—	—
1,3-Dimethoxybenzene[b]	1.45	—	—	—
c1DMeOB	1.90	—	—	—
Chlorobenzene[c]	—	−2.74	—	—
c1ClB	—	<−2.30	—	—
1,3-Dichlorobenzene[c]	—	−2.57	—	—
c1DClB	—	−2.02	—	—

[a] Redox potentials were obtained from ref. 35. [b] Values taken from ref. 36. [c] Reduction potential in DMSO *vs.* SCE, ref. 37. [d] Expressed according to IUPAC convention.

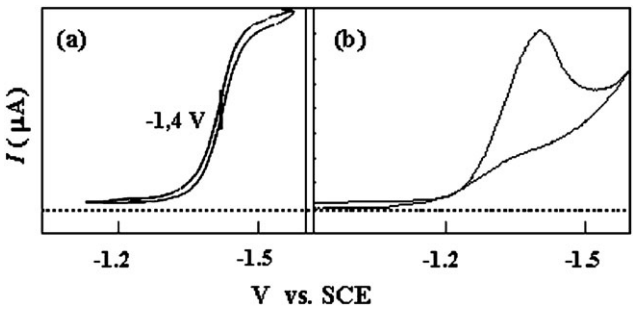

Fig. 2 Cyclic voltagrams for **c1Py** in acetonitrile obtained using a Pt microelectrode (a) and a standard Pt electrode (b).

changes in E_{ox} are in the order of 0.30–0.50 V. The opposite behavior is observed in the reduction potentials. The salts **c1Py**, **c1Naph**, **c1Ant** and **c1DClB** are easier to reduce than the corresponding aromatics. The relative changes in E_{red} are remarkably larger: *ca.* ~0.50–0.70 V. Interestingly, the differences observed in the E_{ox} and E_{red} for the pyrene derivatives **c4Py** and **c1Py** reveal the significance of the aromatic/ammonium group separation in determining the magnitude of the electrostatic effect. The value E_{ox} for **c1MeOB** and E_{red} for **c1ClB** could not be determined because their values are outside the working potential window of the system. Fig. 3 summarizes the shifts in the redox potentials in Table 1: $\Delta E_{red} = E_{Ar/Ar^{-\bullet}} - E_{Salt/Salt^{-\bullet}}$ and $\Delta E_{ox} = -E_{Ar^{+\bullet}/Ar} + E_{Salt^{+\bullet}/Salt^{\bullet}}$.

In principle, the changes observed in the redox properties of the salts, when compared to that of the unsubstituted compounds, could be taken as evidence of an internal field effect. The presence of the charged ammonium group (TAA) exerts a remarkable influence on the development of a second charge in the molecule and a straightforward reasoning can be used to anticipate the direction of observed effects. The generation of the aromatic cation radicals seems to be less favourable when the TAA group is attached to the aromatic ring, while the same group apparently assists the formation of the anion radical. As it is shown in the next section, the magnitude of the changes observed along each direction depends on a number of factors acting simultaneously.

Computational results

The HOMO and LUMOs energies evaluated for **MePy** and the most stable conformations (hereafter referred as conformers of C_1 symmetry) of **c1Py** and **c4Py** are shown in Fig. 4 as solid circles. As expected, by comparing the HOMOs and LUMOs energies of **MePy** and the salts, a remarkable change in the gas phase donor/acceptor capabilities of the salts is observed. The magnitude of the effect increases as the ring–TAA separation decreases. For instance, the ΔI and ΔE_A for **c4Py** are ~1.7 eV and those for **c1Py** are ~3 eV. On the other hand, for a given separation, the TAA group increases both the ionization potentials and the electron affinities to a similar extent. As a consequence, the HOMO–LUMO gap of the salts is nearly independent of the ring–TAA distance. This result is in agreement with the slight changes observed in the E_{00} along the series. Similar

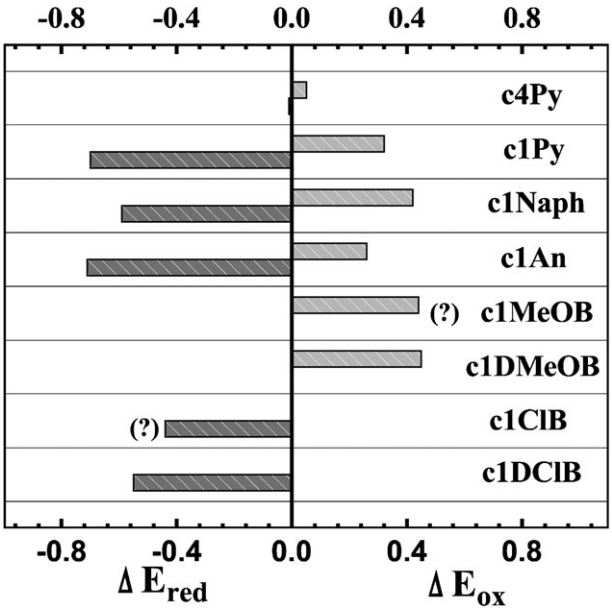

Fig. 3 Summary of the shifts in the electrochemical potentials, ΔE_{red} and ΔE_{ox}, in acetonitrile. The actual ΔE_{red} and ΔE_{ox} for **c1ClBe** and **c1MeOBe** should exceed the values shown in the Figure.

results were found for the naphthalene derivatives as shown in Fig. 6.

In order to estimate the magnitude of the effect exerted by an external (non-bonded) electric field, **c*n*Py** models were calculated. These models were built as a combination of **MePy** plus an array of atomic charges, placed as the TAA group in the **c*n*Py** molecule and chosen to fit the electrostatic potential (ESP) of the group. The results, presented in Fig. 4, show that for the **c1Py** and **c4Py** distances, the HOMO and LUMO shifts are 1.8 and 1.1 eV respectively (compare white *vs.* black circles in Fig. 4). Based on this model, roughly 60% of the overall shift calculated for **c1Py** (~3 eV) and **c4Py** (~1.7 eV) is due to the net electric field. The remaining shift is attributed to the polarization exerted by TAA through the alkyl bridge and to the through-bond orbital coupling between the π system of the chromophore, mainly the σ*(C–C) of the methylene(s) of the bridge, and the σ* orbitals of the TAA group. The contribution of the latter so-called "orbital effect" was estimated from the differences in shifts between the C_1 and C_s conformers of the salts. In the C_s conformers the σ* of the methylene and the aromatic π systems remains orthogonal, as shown in Fig. 5 for **c4Py** and so the Py-bridge–TAA orbital coupling is negligible due to symmetry [the $-(CH_2)_n-$ chain is in the same plane as the pyrene]. In contrast, for the C_1 conformers discussed so far the chain axes lie 83° above the pyrene plane and orbital coupling is optimal (see Fig. 5). The total energy of the C_s conformer lies 9.4 kcal mol^{-1} above of the C_1 conformer in the case of **c1Py** and 2.2 kcal mol^{-1} in the case of the **c4Py** species.[39]

The calculated shifts for the C_s conformers are shown as gray circles on Fig. 4. The slight change observed between C_1 and C_s in **c4Py** (<0.05 eV) indicates that orbital effects are negligible for this compound and that polarization is responsible for the major part of the remaining effect (almost 0.6 eV

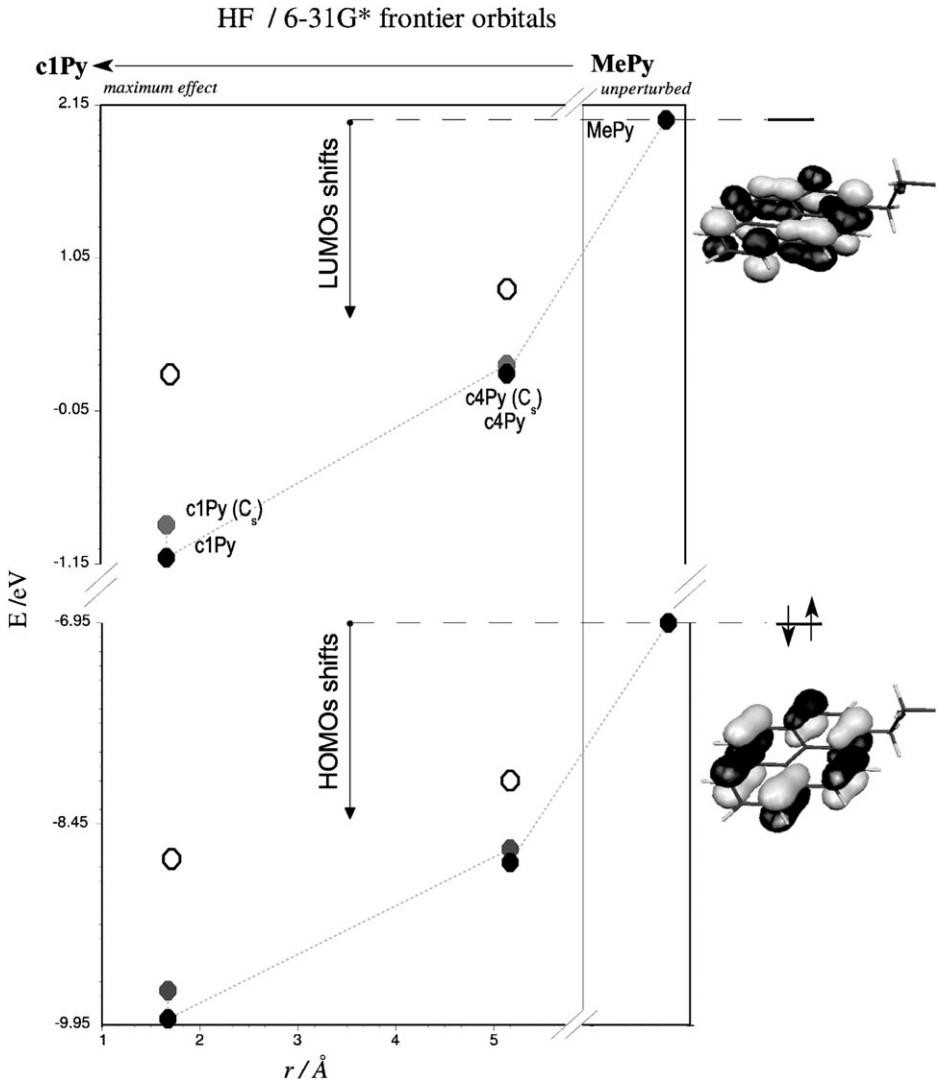

Fig. 4 HOMO–LUMO energies for different separations between the nitrogen of the TAA group and the *ipso*-carbon of the pyrenyl system, *r*. Frontier orbital energies for the C_1 conformers of **MePy**, **c4Py** and **c1Py** species (●); conformers of C_s symmetry of the salts (●); **MePy** exposed to an external (non-bonded) array of charges that reproduces the electrostatic potential of the TAA group (○).

of the whole 1.7 eV shift). For **c1Py** the orbital effect is ~0.3 eV, but even in this case it is fairly small when compared to the 3.1 eV whole shift.

Despite the charge–chromophore orientation changes between the C_s and C_1 conformers (Fig. 5), we have checked that for a given distance, the effect is practically the same whether the TAA group approaches the aromatic system either on the plane (as in the C_s conformers) or above the plane (as in the C_1 conformers). This has been tested with an external (non-bonded) charge model by varying the ring–TAA separation with different axis orientation (details are available as ESI†).

Similar results were obtained for the naphthalene derivatives with a wider variety of chain lengths (see Fig. 6). As can be observed in the figure, the field effect holds even at very long distances (*i.e.* 23 Å for **c16Naph**). Again, the ring–TAA distance is the dominant effect in the MOs energy shifts. The difference in shifts between the C_1 and C_s conformers is 0.26 eV for **c1Naph**, ~0.1 eV for **c2Naph**, and practically negligible for **c4Naph**.[40] A further investigation on the polarization and the role of the alkyl bridge was performed by analyzing the folded conformers of **c7** and **c8Naph**. In these two U-shaped conformers the TAA–naphthyl distance is comparable to that of the linear **c2Naph**, although the TAA and the ring are not close enough to overlap, as checked by NBO analysis.[41] The smaller shift (~0.5 eV) of the folded conformers with respect to **c2Naph** can be mainly attributed to the polarization of the bridge. This is due to the fact that in the linear **c2Naph** the field propagates both through the space and through the bonds of the polarized chain; while in the folded conformers, the chromophore senses the field essentially through the space.

A polar solvent screens the net field sensed by the chromophore and favors charge localization on the TAA and aromatic moieties as illustrated in Fig. 7 for **c4Naph**. While the bridge is smoothly polarized by the TAA charge in the gas phase (Fig. 7a), in a continuum polar solvent a higher charge separation is favored and the aromatic system appears

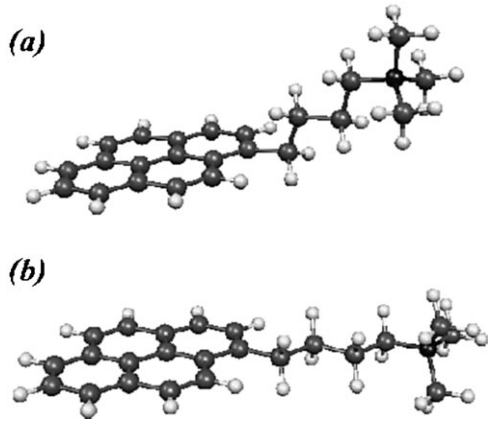

Fig. 5 Structures of the (a) C_1 or totally *gauche* and (b) C_s conformers of **c4Py**, optimized at the HF/6-31G* level.

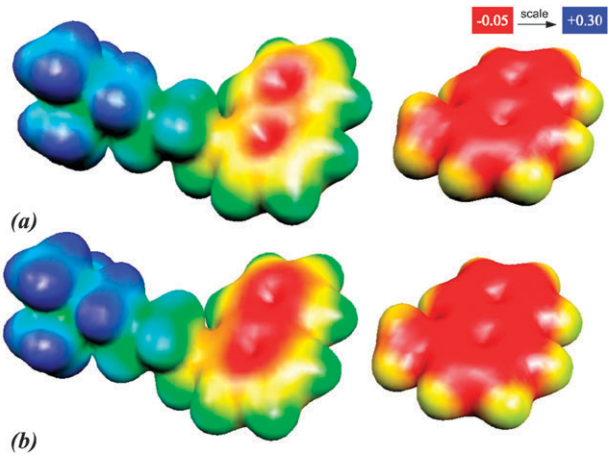

Fig. 7 Calculated electrostatic potentials (ESP) for **c4Naph** and **MeNaph** in the gas phase (a) and in acetonitrile (b).

at a more negative potential, similar to that observed for **MeNaph** (Fig. 7b).

Fig. 8 shows the calculated LUMOs energies for a **c*n*Naph** (***n*** = 1–4) series in acetonitrile. As can be seen, the major part of the electrostatic effects is screened by the polar solvent and the shifts calculated for **c1Naph** decreases from ~3 eV (gas phase) to ~0.8 eV in acetonitrile. The effect practically vanishes for ***n*** > 4, while it still holds for more than 16 methylenes in the gas phase; the shifts for **c4Py** and **c4Naph** were reduced from ~1.7 eV to less than 0.15 eV in acetonitrile. The HOMOs follow a similar trend. Interestingly, the orbital coupling effects for the shortest chain derivatives do not change appreciably (compare gray *vs.* black triangles on Fig. 8) and thus, they acquire relative importance in solution.

The above results illustrate the different contributions that modify the donor/acceptor capabilities of the aromatics. However, in order to estimate the actual changes in the thermodynamic redox potentials of the salts with respect to the reference methylaromatics, the solvation free energies of all oxidized and reduced species (reactants and products) should also be taken into account.

The thermodynamic cycles in Chart 2 can be used to analyze the factors responsible for the electrochemical shifts determined in acetonitrile (Fig. 3). The shift in the electrochemical

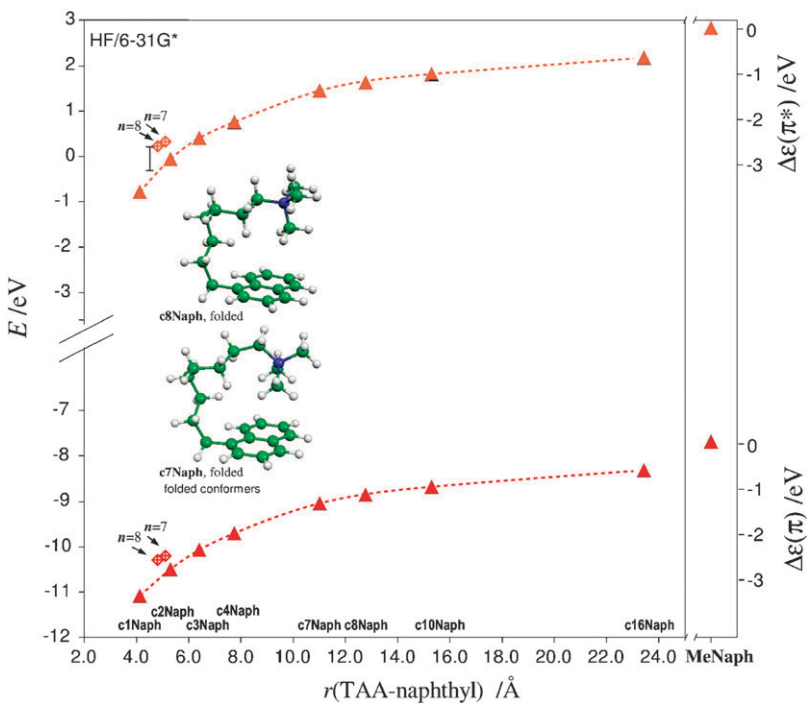

Fig. 6 LUMOs and HOMOs of **c*n*Naph** , n = 1, 2, 3, 4, 7, 8, 10, 16 (C_1 conformers) and **MeNaph** (solid triangles). **c7Naph** and **c8Naph** folded conformers (crossed diamonds). In order to compare the linear and folded species, r is taken between the TAA group and the center of the naphthyl ring.

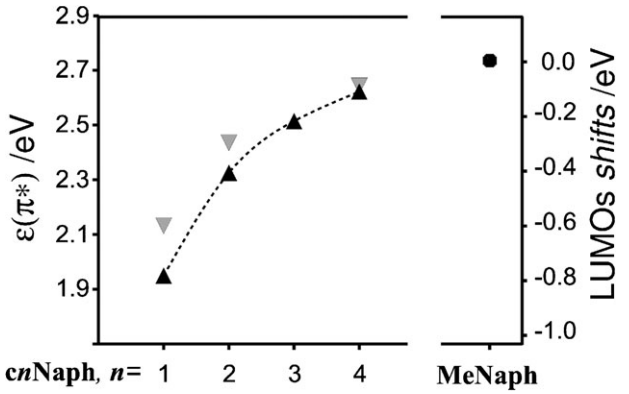

Fig. 8 LUMOs energies for **c*n*Naph** series, C_1 conformers (▲) n = 1 to 4; C_s conformers (▼) n = 1, 2 and 4, in acetonitrile; shifts with respect to the MeNaph (●).

standard reduction potential of **c1Ar** (for which the electrostatic effects are maxima) with respect to the methyl aromatic:

$$\Delta E^0_{\mathrm{red}} = E^0_{\mathrm{Ar/Ar^{-\bullet}}} - E^0_{\mathrm{salt/salt^{-\bullet}}},$$

can be computed by taking the paths shown in Chart 2 and then subtracting the two expressions obtained from cycles in Chart 2a and Chart 2b for the **MeAr** and the **c1Ar**, respectively. This leads to

$$\Delta\Delta G^0_{\mathrm{red}} = -nF\,\Delta E^0_{\mathrm{red}} = -\Delta\Delta G^0_{\mathrm{solv}}(\mathrm{reactants}) - \Delta E_A + \Delta\Delta G^0_{\mathrm{solv}}(\mathrm{red;\ products}).xx \quad (1)$$

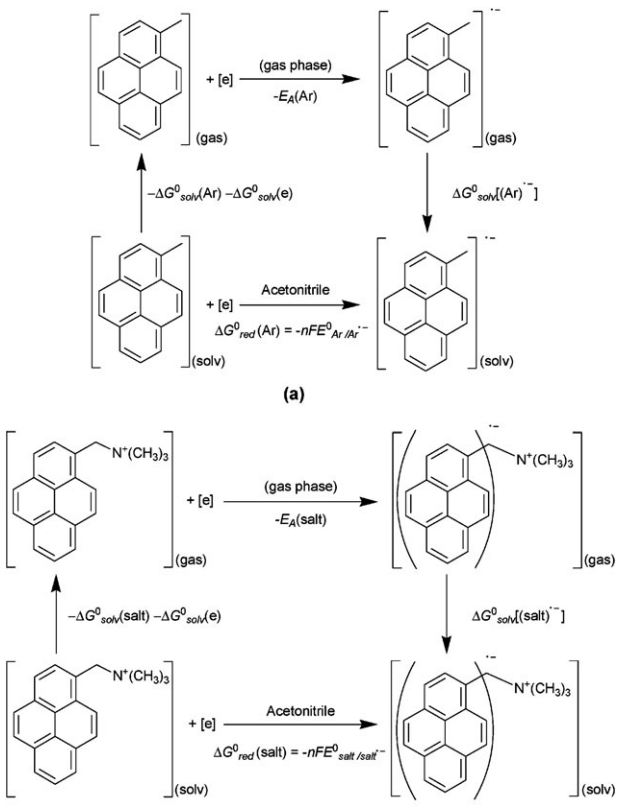

Chart 2

where

$$\Delta\Delta G^0_{\mathrm{solv}}(\mathrm{reactants}) = \Delta G^0_{\mathrm{solv}}(\mathrm{Ar}) - \Delta G^0_{\mathrm{solv}}(\mathrm{salt}) \quad (2a)$$

$$\Delta E_A = E_A(\mathrm{Ar}) - E_A(\mathrm{salt}) \quad (2b)$$

$$\Delta\Delta G^0_{\mathrm{solv}}(\mathrm{red;\ products}) = \Delta G^0_{\mathrm{solv}}(\mathrm{Ar^{\bullet-}}) - \Delta G^0_{\mathrm{solv}}(\mathrm{salt^{\bullet-}}) \quad (2c)$$

Similarly, the following expressions apply to the oxidations:

$$\Delta\Delta G^0_{\mathrm{ox}} = -nF\Delta E^0_{\mathrm{ox}} = -\Delta\Delta G^0_{\mathrm{solv}}(\mathrm{reactants}) + \Delta I + \Delta\Delta G^0_{\mathrm{solv}}(\mathrm{ox;\ products}) \quad (3)$$

where

$$\Delta\Delta G^0_{\mathrm{solv}}(\mathrm{reactants}) = \Delta G^0_{\mathrm{solv}}(\mathrm{Ar}) - \Delta G^0_{\mathrm{solv}}(\mathrm{salt}) \quad (4a)$$

$$\Delta I = I(\mathrm{Ar}) - I(\mathrm{salt}) \quad (4b)$$

$$\Delta\Delta G^0_{\mathrm{solv}}(\mathrm{ox;\ products}) = \Delta G^0_{\mathrm{solv}}(\mathrm{Ar^{\bullet+}}) - \Delta G^0_{\mathrm{solv}}(\mathrm{salt^{\bullet+}}) \quad (4c)$$

The results are summarized on Table 2.[42] The change in the E_A values and I values (gas phase values) are in fact as big as ~3 eV, indicating that the KT values based on the orbital shifts were in the right order of magnitude. The $\Delta E^0_{\mathrm{red}}$ and ΔE^0_{ox}, calculated from eqn (1) and (3), reproduced considerably well (despite the limitations of the model) the direction and magnitude of the experimental redox shifts. An inspection of the data in Table 2 shows that these shifts mainly arise from changes in E_As and Is which are not fully compensated by solvation terms even in a polar medium such as acetonitrile.

The magnitude of the estimated shifts increases in the series **Py**, **An** and **Naph**, which seems reasonable considering that in the smaller aromatics the chromophore is more exposed to the TAA field. However, this trend is not evident in the experimental potentials. The greater shift of the experimental reduction with respect to the oxidation potentials (Fig. 3) has also been found in the calculated values, even though they have shown smaller asymmetries.

Remarks

In summary, the theoretical studies confirm the tendency observed in the experimental redox potentials (Fig. 3). The changes in the donor/acceptor capability of the aromatics linked to the TAA group are the result of a combination of electrostatic, bridge polarization and orbital coupling effects acting together. Both in the gas phase and in a polar medium, the field due to the positively charged TAA enhances the acceptor capabilities of the aromatic ring practically to the same extent to which it precludes its donor strength. These results give further support to the electrostatic catalysis hypothesis in enzymes and could also help to understand the changes in reactivity observed in other systems where the substrate is directly exposed to the field exerted by an ion or dipole; such as in crown ethers, zeolites, and other charged interfaces.

Table 2 Summary of DFT calculations.[a] Calculated changes in the redox properties of the salts with respect to the MeAr and their contributions (Chart 2, eqn (1) and (3))

	ΔG^0_{solv} (Ar or salt)	ΔG^0_{solv} ($Ar^{\bullet+}$) or ($salt^{\bullet+}$)	ΔG^0_{solv} ($Ar^{\bullet-}$) or ($salt^{\bullet-}$)	I	E_A	ΔG^0_{red}	ΔE^0_{ox}
MePy[b]	0.12	−1.30	−1.51	7.00	0.31	—	—
c1Py[b]	−1.38	−5.23	−0.35	9.92	3.47	−0.50	0.49
MePy[c]	0.12	−1.30	−1.51	7.04	0.38	—	—
c1Py[c]	−1.38	−5.23	−0.35	9.96	3.54	−0.50	0.48
MeAn[b]	0.14	−1.32	−1.50	6.94	0.44	—	—
c1An[b]	−1.04	−5.02	−0.08	9.98	3.66	−0.61	0.51
MeNaph[b]	0.12	−1.48	−1.63	7.72	−0.35	—	—
c1Naph[b]	−1.46	−5.75	−0.23	11.05	3.29	−0.66	0.64

[a] All energies in eV and ΔE^0 in V. [b] At the B3LYP/6-31+G** // B3LYP/6-31G* level. [c] Changes in the ion/molecule properties improved at the B3LYP/6-311++G(2d,p) // B3LYP/6-31+G* level.

Acknowledgements

Authors thank Consejo Nacional de Investigaciones Científicas y Técnicas (CONICET-Argentina) and Agencia Nacional de Promoción Científica (FONCYT-Argentina) for financial support. C.A.C. thanks the Secretaría de Ciencia y Técnica de la Universidad Nacional de Río Cuarto. D.M.A.V. and A.B.P. thank the Secretaría de Ciencia y Técnica de la Universidad Nacional de Córdoba (SECYT). The INFIQC is jointly sponsored by CONICET and the Universidad Nacional de Córdoba.

References

1 (*a*) R. W. Taft and R. D. Topsom, *Prog. Phys. Org. Chem.*, 1987, **16**, 1–83; (*b*) S. Ehrenson, R. T. C. Brownlee and R. W. Taft, *Prog. Phys. Org. Chem.*, 1983, **10**, 1–80.
2 Z. F. Bjerrum, *Z. Phys. Chem.*, 1923, **196**, 219.
3 (*a*) J. G. Kirkwood and F. H. Westheimer, *J. Chem. Phys.*, 1938, **6**, 506; (*b*) F. H. Westheimer and J. G. Kirkwood, *J. Chem. Phys.*, 1938, **6**, 513.
4 J. J. Villafranca and T. Novak, in *The Enzymes*, ed. D. S. Sigman, Academic Press, 3rd edn, 1992, vol. 20, pp. 63–94.
5 H. A. McKenzie and F. H. White, *Adv. Protein Chem.*, 1991, **41**, 173.
6 P. A. Frei, S. A. Whitt and J. B. Tobin, *Science*, 1994, **255**, 1927.
7 W. G. J. Hol, P. T. van Duijnen and H. J. C. Berendsen, *Nature*, 1978, **273**, 443.
8 V. V. Lobanov and C. I. Bogillo, *Langmuir*, 1996, **12**, 5171 and references therein.
9 G. Naray-Szabo and G. G. Ferenczy, *Chem. Rev.*, 1995, **95**, 829.
10 G. Naray-Szabo, *Period. Biol.*, 1999, **101**, 325.
11 J. B. Tobin and P. A. Frey, *J. Am. Chem. Soc.*, 1996, **118**, 12253.
12 (*a*) J. Marquet, E. C. Cayón, X. Martin, F. Casado, I. Gallardo, M. Moreno and J. M. Lunch, *J. Org. Chem.*, 1995, **60**, 3814; (*b*) R. González-Blanco, J. L. Bourdelande and J. Marquet, *J. Org. Chem.*, 1997, **62**, 6903–6910; (*c*) F. Casado, L. Pisano, M. Farriol, I. Gallardo, J. Marquet and G. Melloni, *J. Org. Chem.*, 2000, **65**, 322–331.
13 J. Shailaja, P. H. Lakshminarasimhan, A. R. Pradhan, R. B. Sunoj, S. Juckusch, S. Karthikeyan, S. Uppili, J. Chandrasekhar, N. Turro and V. Ramamurthy, *J. Phys. Chem. A*, 2003, **107**, 3187.
14 J. Sivaguru, H. Saito, M. R. Solomon, L. S. Kaanumalle, T. Poon, S. Jockusch, W. Adam, V. Ramamurthy, Y. Inoue and N. Turro, *Photochem. Photobiol.*, 2006, **82**, 123–131 and references therein.
15 (*a*) L. R. Sousa and J. M. Larson, *J. Am. Chem. Soc.*, 1977, **99**, 307; (*b*) A. J. Pearson and W. Xiao, *J. Org. Chem.*, 2003, **68**, 5361.
16 R. E. Gawley, H. Mao, M. Haque, J. B. Thorne and J. Pharr, *J. Org. Chem.*, 2007, **72**, 2187.
17 M. A. Gómez, R. E. Palacios, C. M. Previtali, H. A. Montejano and C. A. Chesta, *J. Polym. Sci., Part A: Polym. Chem.*, 2002, **40**, 901.
18 B. Arnold, L. Donald, A. Jurgens and J. Pincock, *Can. J. Chem.*, 1985, **63**, 3140.
19 T. A. Koopmans, *Physica A*, 1933, **1**, 104.
20 Although the I and E_A obtained by directly applying the KT are not expected to reproduce actual values, the linear relationships of type $I = a\,\varepsilon(\text{HOMO}) + b$ [where ε(HOMO) is the corresponding orbital energy and a and b can be fitted for a given method and basis set; an analogous expression holds for the E_As] are justified and extensively used for correlating experimentalvalues (PES, ETS spectroscopies) and orbital energies, even in the most conflicting cases of compounds having negative electron affinities (see ref. 21, 22 and 23). Nevertheless, in this study we are not concerned with the absolute values of I and E_A but with their differences between the values for the salt ***cn*Ar** and the reference methylaromatic **MeAr**.
21 K. D. Jordan and M. N. Paddon-Row, *Chem. Rev.*, 1992, **92**, 395.
22 R. Stowasser and R. Hoffmann, *J. Am. Chem. Soc.*, 1999, **121**, 3414.
23 See D. M. A. Vera and A. B. Pierini, *Phys. Chem. Chem. Phys.*, 2004, **6**, 2899–2903 and extensive literature cited therein.
24 (*a*) C. Lee, W. Yang and R. G. Parr, *Phys. Rev. B*, 1988, **37**, 785; (*b*) A. D. Becke, *Phys. Rev. A: At., Mol., Opt. Phys.*, 1988, **38**, 3098; (*c*) B. Miehlich, A. Savin, H. Stoll and H. Preuss, *Chem. Phys. Lett.*, 1989, **157**, 200.
25 Taking into consideration the rigidity of the chromophores and the fact that we are considering just the *changes* in the I or E_A, we used their vertical values: *i.e.*, assuming that ΔI or ΔE_A(vertical) $\approx \Delta I$ or ΔE_A(adiabatic).
26 We have already demonstrated that the DFT formalism is reliable enough to reproduce experimental E_As within a few meV, even in the most conflicting case of species having negative electron affinities, see ref. 23.
27 Within the DFT calculations only **MeNaph** has a small negative electron affinity; in this case we have ensured that the conventional (valence) radical anion state has been obtained (ref. 23).
28 M. J. Frisch, G. W. Trucks, H. B. Schlegel, G. E. Scuseria, M. A. Robb, J. R. Cheeseman, V. G. Zakrzewski, J. A. Montgomery, Jr., R. E. Stratmann, J. C. Burant, S. Dapprich, J. M. Millam, A. D. Daniels, K. N. Kudin, M. C. Strain, O. Farkas, J. Tomasi, V. Barone, M. Cossi, R. Cammi, B. Mennucci, C. Pomelli, C. Adamo, S. Clifford, J. Ochterski, G. A. Petersson, P. Y. Ayala, Q. Cui, K. Morokuma, D. K. Malick, A. D. Rabuck, K. Raghavachari, J. B. Foresman, J. Cioslowski, J. V. Ortiz, A. G. Baboul, B. B. Stefanov, G. Liu, A. Liashenko, P. Piskorz, I. Komaromi, R. Gomperts, R. L. Martin, D. J. Fox, T. Keith, M. A. Al-Laham, C. Y. Peng, A. Nanayakkara, C. Gonzalez, M. Challacombe, P. M. W. Gill, B. G. Johnson, W. Chen, M. W. Wong, J. L. Andres, M. Head-Gordon, E. S. Replogle and J. A. Pople, *GAUSSIAN 98 (Revision A.7)*, Gaussian, Inc., Pittsburgh, PA, 1998.
29 (*a*) S. Miertus, E. Scrocco and J. Tomasi, *Chem. Phys.*, 1981, **55**, 117; (*b*) S. Miertus and J. Tomasi, *Chem. Phys.*, 1982, **65**, 239; (*c*) M. Cossi, V. Barone, R. Cammi and J. Tomasi, *Chem. Phys. Lett.*, 1996, **255**, 327.
30 (*a*) B. H. Besler, K. M. Merz, Jr and P. A. Kollman, *J. Comput. Chem.*, 1990, **11**, 431; (*b*) U. C. Singh and P. A. Kollman, *J. Comput. Chem.*, 1984, **5**, 129.

31 (*a*) Within the Gaussian program either the "Pop = MK" or "Pop = ESP" keywords start the MK analysis for obtaining the MK charges (calculations on the salt structure). The "Charge = Angstroms" keyword allows for computing the effect of external charges at given coordinates in Angstroms (applied to the neutral methylaromatics); see also; (*b*) G. G. Hall and C. M. Smith, *Int. J. Quantum Chem.*, 1984, **25**, 881; (*c*) C. M. Smith and G. G. Hall, *Theor. Chim. Acta*, 1986, **69**, 63.

32 (*a*) J. E. Carpenter, PhD Thesis, University of Wisconsin, Madison, WI, 1987; (*b*) J. E. Carpenter and F. Weinhold, *J. Mol. Struct. (THEOCHEM)*, 1988, **169**, 41; (*c*) A. E. Reed, L. A. Curtiss and F. Weinhold, *Chem. Rev.*, 988, **88**, 899; (*d*) *Program NBO 3.1*: E. D. Glendering, A. E. Reed, J. E. Carpenter and F. Weinhold, University of Wisconsin.

33 B. Foster, G. Guillard, N. Mathur, A. Pincock and C. Sehmbey, *Can. J. Chem.*, 1987, **65**, 1599.

34 B. Arnold, L. Donald, A. Jurgens and J. Pincock, *Can. J. Chem.*, 1985, **63**, 3140.

35 H. Been and A. Weller, in *Organic Molecular Photophysics*, ed. J. B. Birks, Willey, New York, 1975, vol. 2.

36 A. Zweig, W. G. Hodgson and W. H. Jura, *J. Am. Chem. Soc.*, 1964, **86**, 4124.

37 J. R. Wiley, E. C. M. Chen, E. S. D. Chen, P. Richardson, W. R. Reed and W. E. Wentworth, *J. Electroanal. Chem.*, 1991, **307**, 169.

38 A. J. Bard and L. R. Faulkner, in *Electrochemical Methods: Fundamental and Applications*, Wiley & Sons, New York, 2nd edn, 2001.

39 Similar conformational energy differences have been obtained for the naphthyl derivatives; these being 8.3, 2.8 and 2.0 kcal for **c1**, **c2** and **c4Naph** respectively. A complete scan of the torsion around the relevant dihedral, monitoring both the total energies and the shifts in the HOMO and LUMO energies, is given for the **c1Naph** in the ESI, Fig. S5†.

40 Complete Table S2 with the gas-phase shifts of the different models available as ESI†.

41 Inspection of the second-order perturbation analysis reveals the absence of interactions (delocalizations) between the π(aromatic)/π*(aromatic) and the σ*(CH)/σ(CH) greater than 0.05 eV. On the other hand, by setting to zero all non-diagonal elements of the Fock matrix involving NBOs of the naphthyl and of the TAA group, the changes in the energy of the HOMO and LUMO are negligible. In NBO analysis this means to "delete" the "through-space" orbital interaction between the TAA and the aromatic. Thus, when comparing the shifts in these particular U-shaped conformers with respect to the linear chain species with similar TAA–aromatic distances, we are viewing different polarization patterns in the bonds of the chain, but we are not simultaneously introducing an important through-space orbital interaction due to the closeness of the groups.

42 The shifts in the standard potentials in acetonitrile (eqn (1) and (3)) as well as their components (eqn (2) and (4)) were calculated at the B3LYP/6-31 + G(d) and B3LYP/6-311 + + G(2d,p) levels of theory for the pyrene derivatives couple **MePy** and **c1Py**. Since the results were essentially equivalent, especially for the most sensitive case of the electron affinity changes, the results for the anthracene and naphthalene derivatives were obtained just at the B3LYP/6-31 + G(d) level.

